

13,06

Heat capacity of mechanically activated BiFeO₃

© R.G. Mitarov², S.N. Kallaev¹, Z.M. Omarov¹, B.K. Abdulvakhidov³, K.G. Abdulvakhidov⁴

¹ Amirkhanov Institute of Physics, Daghestan Federal Research Center,
Russian Academy of Sciences,
Makhachkala, Russia

² Dagestan State Technical University,
Makhachkala, Russia

³ Dagestan State University,
Makhachkala, Russia

⁴ Southern Federal University,
Rostov-on-Don, Russia

E-mail: kallaev-s@rambler.ru

Received March 3, 2025

Revised December 29, 2025

Accepted December 29, 2025

The temperature dependence of the heat capacity of mechanically activated BiFeO₃ ceramics was studied in the temperature range of 120–800 K. It was shown that the excess heat capacity of the mechanically activated ceramics is due to the following factors: dislocations, thermal generation of point defects, energy levels associated with polar displacements of iron and bismuth ions and with a change in the angle between the oxygen octahedra of FeO₆, size effects and an increase in the surface.

Keywords: multiferroics, heat capacity, bismuth ferrite, Schottky heat capacity, mechanically activated ceramics.

DOI: 10.61011/PSS.2026.01.63256.43-25

1. Introduction

Bismuth ferrite BiFeO₃ (BFO) is one of the classical multiferroics exhibiting ferroelectric (Curie temperature $T_C = 1100$ K) and antiferromagnetic ordering (Néel temperature $T_N \sim 640$ K) [1,2]. Due to the effect of magnetoelectric (ME) coupling at room temperature, BFO is a potential material for technological applications such as data and information storage devices, converters, spintronic devices, sensors, and resistive switching elements [3,4]. In the range of temperatures below the Néel temperature T_N , bismuth ferrite has a complex cycloid type spatially modulated magnetic structure which avoids the presence of ferromagnetic properties. A necessary condition for the occurrence of the magnetoelectric effect is the destruction of its spatially modulated spin structure, which can be achieved by various methods, in particular, by alloying BFO with rare earth elements, creating nanostructured and composite materials [5–8]. One of the technical methods of influencing the physical properties of BFO is mechanical activation, which leads to the dispersion of particle sizes to the nanoscale, as well as its saturation with structural defects of a certain concentration and type. Since the particle size of BFO is less than the cycloidal period (62 ± 2 nm), it must transition from the antiferromagnetic to the ferromagnetic state [9].

In this paper, we investigated the heat capacity of mechanically activated BFO over a wide temperature range 100–800 K, including the regions of phase transitions.

2. Experimental procedure

Bismuth ferrite was synthesized by solid-phase reaction. To obtain the composition of BFO, the oxides Fe₂O₃ and Bi₂O₃ (Fe₂O₃ $\geq 99.0\%$, Bi₂O₃ $\geq 99.9\%$, Sigma-Aldrich), which were mixed for two hours in an agate mortar with the addition of ethyl alcohol. The charge was fired in a platinum crucible at a temperature of $T = 1200$ °C for 2 h. Then the resulting material was ground for half an hour and subjected to mechanical activation under pressures of 800 and 1000 MPa between vertically positioned Bridgman anvils, the lower of which rotated with an angular velocity of 0.3 rad/min. A sample in the form of a disk with a diameter of 10 mm and a thickness of about 1 mm was made from the powder activated at a fixed pressure and shear deformation for further ceramic sintering. The sintering of the sample was carried out without the addition of binding additives for three hours at a temperature of $T = 825$ °C.

After the process of powder synthesis and ceramic sintering, the phase composition and structural parameters of each sample were determined using an X-ray diffractometer D2-PHASER (Bruker, Germany) using Cu $K\alpha$ ($K\alpha_1 = 1.54060$ Å and $K\alpha_2 = 1.54443$ Å) radiation in increments of $\Delta 2\theta = 0.01^\circ$ and data acquisition time of $\tau = 0.1$ s per step. The diffraction patterns of the initial and mechanically activated samples were processed by the Rietveld method of full-profile analysis using the Powder Cell 2.3 software package [10]. It was found that the initial and mechanically activated powders at room temperature best correspond to the rhombohedral spatial group R3c.

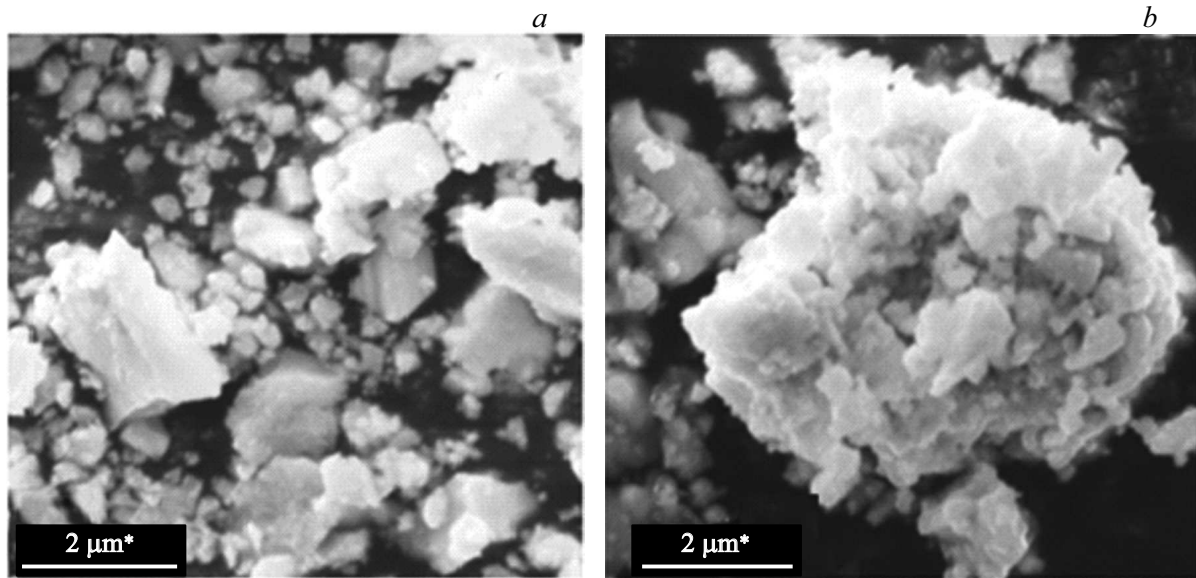


Figure 1. SEM images of bismuth ferrite samples mechanically activated at pressures of 800 MPa (a) and 1000 MPa (b).

However, an additional secondary phase corresponding to $\text{Bi}_{25}\text{FeO}_{39}$ is present in the ceramic samples, but its proportion in the studied samples is insignificant.

Heat capacity was measured by NETZSCH DSC 204 F1 Phoenix differential scanning calorimeter. The sample for measuring the heat capacity is this plate with a diameter of four mm and a thickness of one mm, respectively. The rate of temperature change was 5 K/min. Heat capacity measurement error was lower than 3%.

3. Results and discussions

Figure 1 shows SEM images of mechanically activated bismuth ferrite samples obtained using an FE-SEM Zeiss SUPRA 25 electron microscope. As can be seen from the figure, the samples are characterized by a „loose“ structure and the grain size distribution in the sample is multimodal in the range from 40 nm to 700 nm.

Figure 2 shows experimental data on the heat capacity of BiFeO_3 before and after mechanical activation in the temperature range of 130–800 K. As can be seen from Figure 2, the heat capacity of bismuth ferrite increases significantly after mechanical activation, which indicates the presence of additional heat capacity components that increase with increasing mechanical activation pressure. At the same time, the temperature of the antiferromagnetic phase transition does not shift during mechanical activation, and the heat of the phase transition remains unchanged.

Figure 3 shows the temperature dependence of the excess heat capacity $\Delta C = C_p^m - C_p^n$, which was defined as the difference between the experimental dependences $C_p^m(T)$ of mechanically activated and C_p^n of non-mechanically activated bismuth ferrite samples. A similar dependence of the abnormal heat capacity on temperature $\Delta C(T)$ also

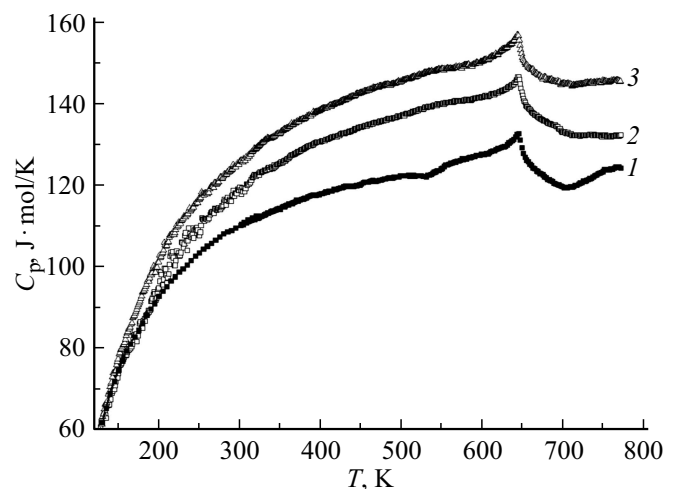


Figure 2. Temperature dependences of the heat capacity C_p before (1) and after mechanical activation of the multiferroic BiFeO_3 at various pressures: 2 — 800 MPa and 3 — 1000 MPa.

exists for nanostructured SmFeO_3 obtained by mechanical activation under a pressure of 200 MPa [11].

Let's consider what additional components of the heat capacity may appear during mechanical activation of the multiferroic BiFeO_3 . According to Ref. [12], high concentration of defects leads to the increase in the heat capacity of nanostructured BiFeO_3 and thermodynamic property smearing in the phase transition region. Mechanical activation of BiFeO_3 leads to the appearance of point defects and dislocations [13]. If the crystal lattice defects are generated thermally, then the defect generation energy also provides additional contribution to the heat capacity of BiFeO_3 ceramic crystal lattice. Therefore, it can be assumed

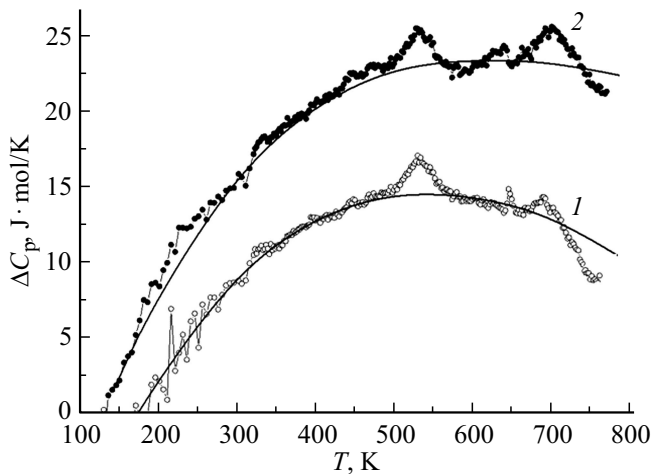


Figure 3. Temperature dependence of the anomalous component of the heat capacity $\Delta C = C_p^m - C_p^n$. 1 — 800 MPa and 2 — 1000 MPa, solid line — the result of approximation by the expression (1).

that the excessive heat capacity in samarium ferrite is caused by thermal generation of point defects and dislocations.

The presence of another heat capacity component in bismuth ferrite may be related to ions that can occupy different (several) structurally equivalent positions separated by energy barriers ΔE_1 , ΔE_2 . The authors of Ref. [14] attribute the appearance of such states separated by energy barriers ΔE_1 and ΔE_2 from the ground state to changes in the crystal lattice parameters due to polar displacements of iron and bismuth ions, as well as to changes in the angle between oxygen octahedra FeO₆ with increasing temperature. Calculations show that the anharmonic component of the heat capacity is less than two percent of the total heat capacity BiFeO₃, and therefore it can be assumed that $C_p = C_v$. The anharmonic component of the heat capacity of a non-mechanically activated bismuth ferrite sample was estimated using literature data on the linear expansion coefficient Bi_{1-x}La_xFeO₃ [15] and the volume compressibility modulus of ceramics Pb(TiZr)O₃ [16], similar in structure to BiFeO₃. However, anharmonic effects can increase in mechanically activated bismuth ferrite samples due to the small particle sizes, and, consequently, the anharmonic component of the heat capacity in them is greater than in an unmechanically activated bismuth ferrite sample [17]. The increase in the heat capacity of mechanically activated bismuth ferrite samples may also be due to the dimensional effect and an increase in surface area during mechanical activation [17].

The isolation and calculation of the above-listed heat capacity components initiated by mechanical activation is difficult due to the lack of necessary data for such a calculation.

The analysis of the temperature dependence of the additional heat capacity ΔC (Figure 3) allows interpreting it as a Schottky anomaly for three-level states. For a three-

level system, the Schottky heat capacity is calculated using the formula [11]:

$$C_{sch} = R \cdot \left[D_1 \cdot \left(\frac{\Delta E_1}{kT} \right)^2 \cdot \exp\left(-\frac{\Delta E_1}{kT}\right) + D_2 \cdot \left(\frac{\Delta E_2}{kT} \right)^2 \exp\left(\frac{\Delta E_2}{kT}\right) \right] / \left[1 + D_1 \cdot \exp\left(\frac{\Delta E_1}{kT}\right) + D_2 \cdot \exp\left(-\frac{\Delta E_2}{kT}\right) \right]^2, \quad (1)$$

where D_1 and D_2 is the ratio of the multiplicities of the degeneracy of the levels.

By comparing the heat capacity calculated by the formula (1) (solid line in Figure 3) and the experimentally isolated excess heat capacity ΔC , model parameters were obtained for mechanically activated BiFeO₃ at a pressure of 800 MPa — $D_1 = 4.012$, $D_2 = 0.740$, $\Delta E_1 = 0.933$ eV and $\Delta E_2 = 0.257$ eV and 1000 MPa — $D_1 = 7.530$, $D_2 = 0.375$, $\Delta E_1 = 0.401$ eV and $\Delta E_2 = 0.632$ eV. Agreement of the experimentally isolated anomalous heat capacity ΔC with the calculated formula (1) C_{sch} is good enough (Figure 3). It should be noted that the observed λ anomalies in the temperature range of 670 and 558K may be due to structural phase transitions.

4. Conclusion

Thus, based on an experimental study of the heat capacity of bismuth ferrite in a wide temperature range, it was found that the excessive heat capacity of mechanically activated samples may be due to: 1) thermal generation of point defects and dislocations that occur during mechanical activation; 2) transitions between energy levels associated with polar displacements of iron and bismuth ions, as well as with changes in the angle between oxygen octahedra FeO₆ with increasing temperature; 3) an increase in the anharmonic component of the heat capacity; 4) an increase in surface and dimensional effects.

Conflict of interest

The authors declare that they have no conflict of interest.

References

- [1] A.K. Zvezdin, A.P. Pyatakov. UFN **182**, 6, 594 (2012) (in Russian).
- [2] S. Falahatnezhad, H. Maleki, A.M. Badizi, M. Noorzadeh. J. Mater. Sci. Mater. Electron. **30**, 15972 (2019)
- [3] Y.M. Abbas, A.B. Mansour, S.E. Ali, A.H. Ibrahim. J. Magn. Magn. Mater. **482**, 66 (2019)
- [4] W. Eerenstein, N.D. Mathur, J.F. Scott. Nature **442**, 759 (2006)
- [5] C.E. Camayo, S. Gaona, F.V. Raigoza. J. Magn. Magn. Mater. **527**, 167733 (2021).

- [6] G.Le Bras, P. Bonville, D. Colson, A. Forget, N. Genand-Riondet, R. Tourbot. *Phys. B Condens. Matter* **406**, 1492 (2011).
- [7] S. Atiq, M. Faizan, A.H. Khan, A. Mahmood, S.M. Ramay, S. Naseem. *Results Phys.* **12**, 1269 (2019).
- [8] F. Pedro-García, F. Sánchez-De Jesús, C.A. Cortés-Escobedo, A. Barba-Pingarrón, A.M. Bolarín-Miró. *J. Alloys Compd.* **711**, 77 (2017).
- [9] I. Sosnowska, T.P. Neumaier, E. Steichele. *J. Phys. C Solid State Phys.* **15**, 4835 (1982).
- [10] I. Dmitrenko, K. Abdulvakhidov, A. Soldatov, A. Kravtsova, Zh. Li, M. Sirota, P. Plyaka, B. Abdulvakhidov. *Applied Physics A* **128**, 1128 (2022).
- [11] R.G. Mitarov, S.N. Kallaev, Z.M. Omarov, M.S. Khizriev, K.G. Abdulvakhidov. *FTT* **64**, 5, 599 (2022) (in Russian).
- [12] A.P. Levanyuk, V.V. Osipov, A.S. Sigov, A.A. Sobyenin. *ZhETF* **76**, 345 (1979).
- [13] S.N. Kallaev, N.M-N. Alikhanov, Z.M. Omarov, S.A. Sadykov, M.A. Sirota, K.G. Abdulvakhidov, A.V. Soldatov. *FTT* **61**, 1358 (2019) (in Russian).
- [14] D.C. Arnold, K.S. Knight, F.D. Morrison, Ph. Lightfoot. *Phys. Rev. Lett.* **102**, 027602 (2009).
- [15] A.A. Amirov, A.B. Batdalov, S.N. Kallaev, Z.M. Omarov, I.A. Verbenko. *FTT* **51**, 1123 (2009) (in Russian).
- [16] J. Ronguette, J. Haines, V. Bornand, V. Bornand, M. Pintard. *Phys.Rev. B* **65**, 214102 (2002).
- [17] A.I. Gusev. *Nanomaterialy, nanostruktury, nanotekhnologii. Fizmatlit, M.* (2009). p. 416 (in Russian).

Translated by A.Akhtyamov